UDC: 579.65:004.89 https://doi.org/10.15407/jai2024.02.062

Yu. Gorgo[1], I. Hretskyi[2], P. Nejedlik[3], A. Prigancova[4], E. Kalinichenko[5], E. Gromozova[6]

[1,5]National Technical University of Ukraine "Igor Sikorsky Kyiv Polytechnic Institute", Ukraine
37, Prospect Beresteiskyi, Kyiv, 03056

[2,6]D.K. Zabolotny Institute of Microbiology and Virology of the National Academy of Sciences of Ukraine, Ukraine
154, Akademika Zabolotnogo St., Kyiv, 03143

[3,4]Earth Science Institute of the Slovak Academy of Sciences, Slovakia
9, Dubravska cesta, Bratislava, 840 05

[1]yugorgo@ukr.net

[1]https://orcid.org/0000-0002-7353-7162
[2]https://orcid.org/0000-0001-8646-0574
[3]https://orcid.org/0000-0003-4417-3758
[6]https://orcid.org/0000-0002-5161-7727

QUANTITATIVE ESTIMATES OF THE METACHROMASIA REACTION OF VOLUTIN GRANULES OF YEAST USING NEURAL NETWORKS

Abstract. The metachromatic coloration of volutinous granules of the yeast Saccharomyces cerevisiae is one of the indicators of the influence of sharp geomagnetic field (GMF) perturbations. The metachromasia reaction is based on the aggregation of dye molecules in interaction with inorganic polyphosphates, which are components of volutinous granules. To determine the characteristics of the geomagnetic field that cause the appearance of different colors of the metachromasia reaction, it is necessary to simultaneously monitor this reaction and changes in the GMF. High-quality monitoring is possible with rapid automated counting of cells with all possible color changes during the metachromasia reaction. The aim of the work was to develop a neural network architecture for recognizing and quantifying color changes and heterogeneity in real time during monitoring of the metachromasia reaction of volutinous granules of the yeast S. cerevisiae, which is necessary for further determining their correlations with changes in the geomagnetic field of different intensities. A program based on a nonrecursive labeling algorithm was created to count the number of cells in the study groups. In the course of the work, the software of two neural network architectures was compared to determine the best results in recognizing and quantifying yeast cells with different colors during the volutinous granule metachromasia reaction. It was determined that the Unet architecture type coped with the tasks of cell classification and segmentation much more efficiently than the Inception v3 architecture. The average relative error for automatic recognition of all cell groups was 3.85%, and the maximum relative error was 4.56%. The performance of the neural network was 89.9% when detecting cell segmentation and 86.4% when detecting color differences in the metachromasia reaction.

Keywords: metachromasy, geomagnetic field, volutin granules, neural networks, yeast.

Introduction

Due to significant climate change and the impact of space weather on biota, it is an urgent issue to identify biological systems that are sensitive to changes in the environment [1-5]. This can be useful in the development of biosensor devices that are sensitive to sudden changes in geophysical factors [6, 7]. It has been established that the color change of the metachromatic reaction of volutinous granules of the yeast *Saccharomyces cerevisiae* is a potential bioindicator of geomagnetic field perturbations [4, 8-10]. In this case, the phenomenon of metachromasia is manifested in a characteristic color change (different from the color of the "methylene blue" dye) in the process of staining yeast volutinous granules. It has been shown that the main colors of metachromasia are largely due to the aggregation of dyes, which is induced by concentration and chromotropic effects that depend on the electromagnetic background [11, 12].

An important task related to the study of the number of cells with changes in the color of the metachromatic reaction of volutinous granules during geomagnetic field perturbations of different strengths is to develop methods for rapidly accounting for such changes. The manifestation of the color of the metachromatic reaction cannot be measured by the colorimetric method, since aqueous dye solutions do not obey Beer's law [5]. Technologies for manual visualization of changes in cells are still widely used in cell counting methods. However, they have a number of disadvantages, such as low sensitivity and specificity, low reproducibility of results, and a long time to detect and evaluate changes in cells [5, 13]. Such methods

of assessing changes in the color of the metachromatic reaction are not capable of fast and automatic data processing during monitoring studies, which are necessary to determine the correlations between changes in the color of the metachromatic reaction and geomagnetic disturbances [4, 5, 13, 14]. For high-quality monitoring, it is necessary to quickly automate the counting of cells with all possible color changes during the metachromatic reaction.

It is known that the reorganization of electronic interactions within the aggregates leads to a shift in the resonant frequency, which is manifested in 3 types of color changes in the metachromatic reaction [15].When staining, we distinguish between:- α-metachromasia (non-metachromatic color), β-metachromasia (weak purple color, intermediate between blue and red), and γ-metachromasia (strong positive red color) [4, 15].These colors indicate whether the dye is in one of the following forms: a dye monomer (α-metachromatics), a short polymeric dye of two and three or more components (β-metachromatics), or a structurally more complex polymeric dye (γ-metachromatics) [5, 12, 17].However, yeast volutin grains often contain segments of heterogeneity where the color of the metachromasia reaction changes [18, 19], which is manifested by the appearance of red areas within still blue volutin granules [5, 12]. In addition, there are a certain number of cells in which no color change was observed during the metachromasia reaction due to the absence of a reaction, and they must also be counted. Therefore, for qualitative monitoring studies, it is necessary to recognize and quantify 5 types of changes in cells during the metachromasia reaction: 3 types of cell color changes, cells with heterogeneity, and cells with no reaction [20, 21].

The use of neural networks with certain training makes it possible to automatically and in real time assess changes in color in cells and take them into account during the metachromasia reaction [22-25]. Such an approach to assessing changes in the number of cells with different colors is an effective way to determine the degree of influence of geomagnetic field perturbations of different intensities on the metachromatic reaction of volutin granules of the yeast S. cerevisiae.

The aim of this work was to develop a neural network architecture for recognizing and quantifying color changes and heterogeneity in real time when monitoring the metachromasia reaction of *S. cerevisiae* volutinous yeast granules of UCM Y-517 and determining their correlation with changes in the geomagnetic field of different intensities.

Materials and methods

The dataset of twenty photographs of cells *S. cerevisiae* UCM Y-517 colored in methylene blue (by Lefler) [5] is used in the paper. A photo editor, "Corel PHOTOPAINT X6," was utilized to process photos. Taking into account the peculiarities of the dataset obtained, the methods of pre-processing images for segmentation of cells with volutin granules according to different types of color metachromasia response and cell classification according to their classes of presence and absence of metachromasia, respectively, have to be determined [26, 27]. In order to count the number of cells with a particular characteristic (index k in 5 degrees) of the volutin granule metachromasia reaction (S), the following formula was used: $S = \sum_{k=1}^{5} {}^{D_k}/_{N_k}$, where D_k is the presence of a cell metachromasia reaction of the k-type, and N_k – is the number of determined cells of a given type.

When building the NNs, it was necessary to choose the network architecture type, select learning scales, set the number of inputs and transfer functions of the used neurons and their interconnection, and, finally, determine the outputs of the particular network [28 - 30]. For this purpose, a convolutional NN was selected using the Python programming language and the Keras open NN library [31 - 33]. The Inception v3 and Unet models were applied when modeling the architecture of the particular NN. Those were earlier developed for the problems of classification and segmentation of objects in the image [34,35] and for cell segmentation in medical images [36, 37], respectively.

To solve the tasks of cell segmentation and their classification into two classes of presence and absence of metachromasia, the program codes for the NN were proposed

according to the two NN architectures. Then the NN was trained using the obtained data. In addition, the effectiveness of trained NNs was tested using test data. Then, as a first step, cells were classified and segmented by applying a trained NN. The number of cells was calculated using a non-recursive markup algorithm as a second step [38, 39]. The statistical calculations of the color characteristics of yeast cells with a detected metachromatic reaction and cells without this reaction or of the NN efficiency for two NN architecture types were performed separately using the MS Excel 2010 program.

Further, it was necessary to build a deep convolutional NN [40 - 42] designed specifically for processing input images of volutin yeast granules. The main idea of this process was to supply the usual network with additional sequential layers where increment sampling operators replace union operators. Hence, these sequential convolutional layers increase the output resolution due to increased digitization [43, 44]. The high-resolution functions were joined with digitized outputs via feedback to perform cell localization. It enables training a sequential convolutional layer to get a more accurate result using additional information [45, 46].

The Inception architecture was used to perform the mentioned operation. It consists of two main blocks. The first block determines the NN features and plays the role of an extractor of functions. The block ensures compliance with the templates by applying convolution filtering operations to fulfill this function. The first aggregate layer filters the image using multiple kerners and returns "object maps, " normalized with the activation function or resized. Recognition of objects on the input layer was represented as a three-dimensional grid, the dimensions of which depend on the input image, according to the formula:

$$I_n = W \cdot H \cdot D,$$

where I_n is the input NN layer size, W and H are the widths and the height of the input image, respectively, D is the number of color channels of the image [47]. A maximizing aggregation layer was selected with 2×2 filters used in increments of 2, which reduces the sampling of each section of the input depth twice for both width and height, discarding 75% of the excitations. It is worth stressing that each operation takes the top acts over four numbers, keeping the depth size unchanged [48].

The NN architecture of GoogleNet Inception v3, trained on about a million images and about a thousand object classes, was taught on our dataset using training with a teacher [37, 42, 49, 50]. The transfer learning method is used for the NN. This method allows for retraining the last level of the existing model in order to significantly reduce the learning time and size of the necessary data chosen. This paper uses the Inception v3 model trained for the ImageNet Large Visual Recognition Challenge on 2012 [51] data as a pre-trained model.

The NN based on the Unet architecture consists of a narrow path corresponding to the convolutional NN's type and architecture. That is represented by reapplying two 3x3 convolutions, followed by a layer of offcut line nodes (ReLU – Rectified Linear Unit) and the 2x2 aggregation operation in increments of 2 to reduce the resolution [42]. ReLU uses the nonviolent transmitting function f(x) = max (0, x) for these operations to fulfill this step. The ReLU correctional layer enhances the nonlinear properties of the decision-making function and NN as a whole without affecting the recipe fields of the convolutional layer. We have changed this architecture to work with a few learning images and give more accurate segmentations.

Because of very little training data, we have used artificial data magnification, applying deformations to existing learning images. It allows the NN to study the invariance of such deformations, which is essential since, in biomedical segmentation, deformations are the most common variations in tissues and cells. The importance of increasing the data for invariance teaching in uncontrolled learning of properties was shown in [42].

Results

In this paper, the analysis of the dataset of 20 images was carried out. The dataset features were established, considering the

proper choice of methods for pre-processing of images. A training sample of photographs was prepared after pre-processing the initial dataset of images. To reduce the requirements for computational power, all images were transformed from a size of 1600x1200 pixels to that 224x224 pixels. For the NN architecture types based on the Inception v3 and Unet models training masks of individual segmented cells were created using the Corel PHOTOPAINT X6 photo editor (Fig. 1). The NN training for cell segmentation and classification according to two features of the cell reaction, namely presence and absence of metachromasia, was carried out.

The analysis of the metachromasia reaction of yeast cells S. cerevisiae. Python programming language created the NN based on the Inception v3 architecture. The NN code was developed to recognize cell segmentation according to metachromasia's presence or absence. Then the NN training with testing the effectiveness of the trained NN was carried out using test data. An average brightness for the image portion was determined first (Fig. 2a). Then, the image portions of a lower than average brightness were determined, those being surrounded by pixels of a higher than average brightness. Binarization for segmentation of each cell was applied (Fig. 2b). Further to that; the NN is going to carry out the classification of segmented cells denoting the corresponding class in color: "presence of metachromasia" - red, "absence of metachromasia" – blue (Fig. 2c).

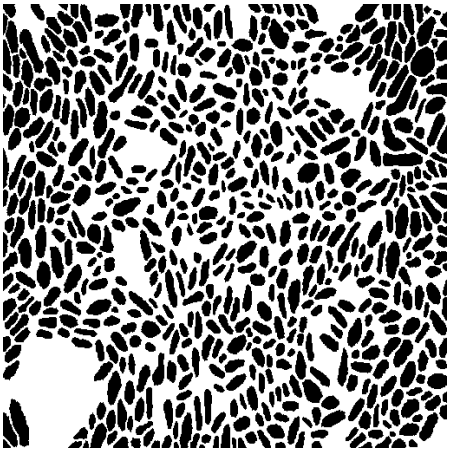

Figure 1. Training mask for teaching the NN

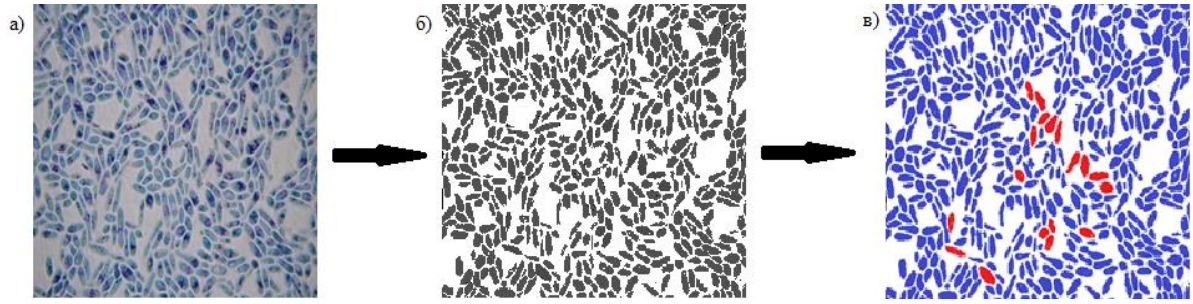

Figure 2. NN (based on Inception v3 architecture) input and output images: a) input image, b) image with segmented cells, c) image with classified cells

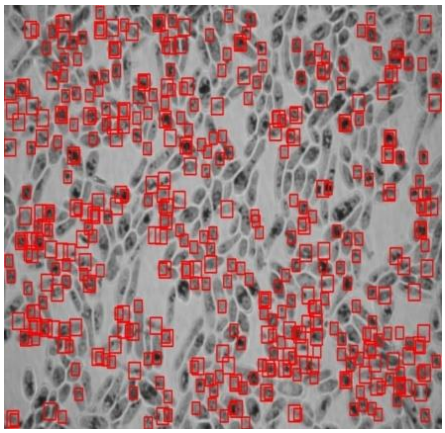

Figure 3. The image with identified cells

After the trained NN already segmented and classified cells, the number of cells with a metachromasia reaction can be calculated using a non-recursive markup algorithm. The NN based on the Inception v3 architecture analyzes the image and produces results of the analysis of the neuron in the form of red rectangles by which the detected cells are visualized (Fig. 3). On top of that, an analysis of the NN effectiveness was carried out using methods of mathematical statistics. As visible in Fig.3, the NN based on the Inception v3 architecture could not isolate all cells with existing features. The program effectively performs cell segmentation but makes errors at the next stage of cell classification. When the volutin granules of cells do not have a clear blue color, the NN classifies them incorrectly as "metachromasia." This type of architecture needs sufficient detection accuracy. It requires significant computing resources (highly time-consuming) since many neural layers are used. The NN efficiency was found to be 80.3%, which means an insufficiently accurate cell separation and the necessity to increase training and work efficiency data to receive satisfactory results [52, 53]. Naturally, to continue NN training and improve the methodology of pre-processing of images, particularly reducing noise, is the way to distinguish an image according to the actual size of pixels instead of approximating it as a whole.

To address these difficulties, it was decided to conduct the NN (based on the Unet architecture) training using training images and training masks of segmented cells. The main difference between the Unet architecture and the Inception v3 architecture is in the way of teaching and visualization result. The Unet NN can carry out adequate cell segmentation in the images and highlight the silhouettes of objects by binarization. The data obtained were presented in the dataset of 20 images. Initially, a dataset with a volutin granules metachromasia reaction in yeast cells *S. cerevisiae* was separated into two sets - the training set and the set for verification. Preliminary processing and expansion of the image, which included standardization and scaling of the input image to improve the dataset transfer quality, was carried out. Training masks of segmented cells were created using the Corel PHOTOPAINT X6 photo editor.

In preliminary data preparation, the images' main shortcomings were leveled. Those are the blurred contours and boundaries of cells, the presence of dye spots in the background, the lack of precise color gradation depending on the type of metachromasia reaction, differences between cell sizes, and too large cell size. These shortcomings increase noise and reduce the data processing efficiency. In order to expand the dataset, the images were adapted to the size of the NN model; mask fragments of 224x224 pixels were created from a size of 1200x1600 pixels. To improve the model's accuracy, images of individual cells were added to the dataset to move from the overall rating format to the specific one.

As noted above, two datasets were used in the paper: a training set and a set for verification. A dataset fulfilled the verification set's role of adjusting the model's hyperparameters for training.

When creating the NN based on Unet, the Python 3.7 language was used, and the NN code was developed. It improved the NN efficiency. The code distinguished three stages in the process of analyzing the metachromasia reaction. At first, the segmentation of yeast cells in the image was carried out by the NN, followed by the classification of cells by the degree of the color of the reaction of the volutin granules of each cell in the image. The degree of metachromasia reaction for the entire image was then estimated along with checking the total number of cells and the number of cells for which the metachromasia reaction was present. In other words, to classify cells the image with segmented cells without classification was obtained before obtaining the image with cells classified as "presence of metachromasia" and finally that of "absence of metachromasia".

Counting the number of cells. To calculate the number of cells in 5 considered groups, the program for counting the number of cells has been created. It is based on a non-recursive markup algorithm. This algorithm works via the utilization of a corner-like shape so-called the ABC mask [34, 54] (Fig. 4). To

find out specific color components, the passage of this mask through the images of cells takes place from left to right and from top to bottom.

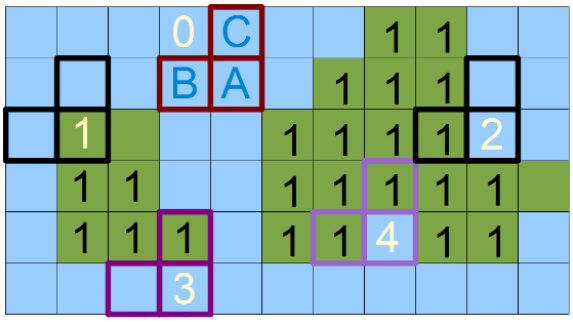

Figure 4. ABC mask and direction of sequential image (its green part) scanning

Five possible positions of the mask from top to bottom on color images of metachromasia analyzed are shown in Fig. 4:

- position 0, when all three components of the mask are not marked (color reaction of metachromasia is absent) – in this case, a pixel is skipped (no mark is created);
- position 1, when only the color component A (α-metachromasia) is marked – in this case, a mark 1 is created;
- position 2, when only the component B (β-metachromasia) is marked – in this case, pixel A is marked as 2, which is located in B;
- position 3, when only the component C (γ-metachromasia) is marked – in this case, pixel A is marked as 3, which is located in C;
- position 4 means that the labels (object numbers) B and C are equivalent, and pixel A can be labeled as B or C. If the value B is not equal to the value, C, all already processed pixels labeled as C are relabeled in B and renumbered.

Then the number of cells, namely the total and number of cells for each of the three types of metachromasia reaction, is counted using a non-recursive markup algorithm.

After the dataset analysis, the network segments individual yeast cells, defines the area of interest where the metachromasia reaction can be detected, and counts cells with an apparent metachromasia reaction. The method of automatic semantic segmentation was used for image segmentation. Using this approach, the model works with a set of objects in which each pixel is labeled. That is used in further analysis to be carried out (Fig. 5).

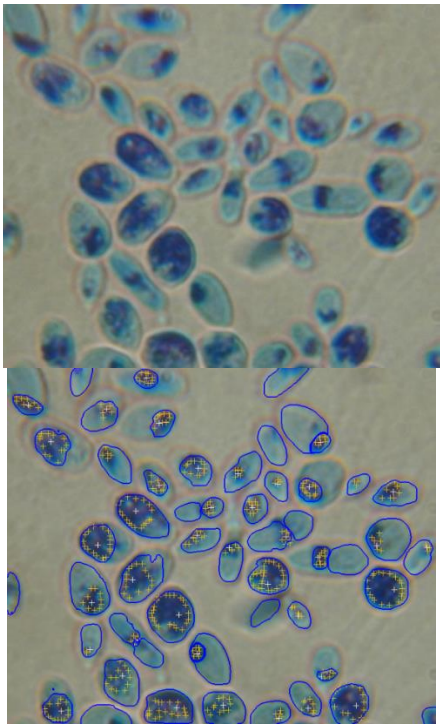

Figure 5. Comparison of the input test image (left) with the output image given by the NN based on the Unet architecture

A comparison of the cell color background when each pixel is assigned a number was used in this analysis. These numbers helped indicate the area in which the phenomenon of metachromasia was detected. Such zones stood out with yellow marks, significantly narrowing the range of reactions to be searched for the color. The white marks determined the most contrasting pixel inside the range of yellow marks, which is necessary for further counting the number of cells with metachromasia. Attaching marks in the form of dots or crosses avoided blurring the data with a rectangular frame superimposed on each other, thereby reducing the result's accuracy (see Fig. 3).

The Inception v3 NN model was used to count the total number of cells and also to count separately both the number of cells for the present (3 types of images corresponding to 1 – α-metachromasia; 2 - β-metachromasia; 3 - γ -metachromasia, as mentioned above) and absent metachromasia reaction of volutin granules of yeast *S. cerevisiae*. Results for manual and automatic methods are presented in Table 1.

Table 1. Manual and automatic counting of the number of cells in datasets with (three types of metachromasia reaction) and without metachromasia

Type of metechro-masia image in cells	Total number of counted cells		Number of cells with "metachromasia"		Number of cells with "no metachromasia"	
	Manual	Automatic	Manual	Automatic	Manual	Automatic
1	363±11	374±10	16	20	347	354
2	474±22	496±23	26	28	448	473
3	324±13	337±14	34	41	290	296

The average relative error value for automatic recognition of these three groups of cells (manifesting three types of metachromasia reaction) is 3.85%, the maximum relative error being 4.56%. The Inception v3 NN model has coped with the recognition of cell contours. However, difficulties have arisen with recognizing cells manifesting a metachromasia response. It was influenced by the insufficient image quality, insufficient quality of their processing, and the amount of data in datasets. The training of the Unet NN model made it possible to determine the number of segments with small isles of the metachromasia reaction and the number of segmented cells without such a reaction in segments (Table 2).

Table 2. The Unet NN results of determination of segments with three types of metachromasia reaction in cells

Type of metachromasia image in cells	Number of segments with metachromasia (3 types of reaction) in cells			Number of segments without metachromasia in cells		
	Manual	Automatic	Relative error, %	Manual	Automatic	Relative error, %
1	0	0	-	27	30	10
2	5	9	20	16	18	11
3	36	39	7,6	43	47	9,3

Discussion

As can be seen from Table 1, in cells with type 1 metachromasia reaction, all detected segments were free of metachromasia. In the case of the second type of reaction, a few segments were found with the metachromasia reaction and only a few segments without metachromasia in the images of segmented cells. The most significant number of with and without apparent metachromasia responses were easily identified on images with the third type of reaction (Table 1). At the same time, some of the identified segments did not have information about the color change of the metachromasia reaction. However, it should be noted that the number of cells with accurate results obtained by registration using a neural network is higher than that obtained by manual registration [12, 30, 52].

The study revealed the advantages of the automatic method for processing metachromasia reaction data. The average relative error for automatic recognition of all groups of cells was revealed to be 3.85%, and the maximum relative error was 4.56%. The neural network can be used to automate the estimation of the number of cells and the intensity of their coloration in monitoring studies of the impact of geophysical disturbances on the metachromatic reaction of volutinous yeast granules [4, 5].

Training of the neural network model allowed us to determine the number of segmented cells with the presence of the "metachromasia reaction" in the segments and the number of segmented cells with the absence of such a reaction in the segments (Table 2). The average relative error was 10.1% in the identification of segments in cells without a metachromasia reaction and 13.8% in the identification of segments with a metachromasia reaction (Table 2). The developed program using the Inception v3 and Unet architectures for detecting and processing color changes in the metachromatic reaction showed that the model of such a convolutional neural network effectively copes with the tasks

of cell segmentation recognition at the level of 89.9%, and when detecting the types of metachromatic reaction in the segments, the recognition rate was 86.2%. This indicates the effectiveness of the NN at a sufficient level of >80% [55] to detect color changes in the metachromatic reaction using the applied specific neural network training.

Moreover, the great advantage of the automatic method of counting the cells is its higher accuracy and rate of calculations, which is extremely necessary for monitoring studies of cell transformations and in further application of data obtained for interdisciplinary research [5, 19, 22].

The neural network coped with the recognition of cell contours, but there were difficulties with the recognition of cells with the absence and presence of a metachromasia reaction. This was due to poor image quality, insufficient processing, and the amount of data in the datasets [24, 42, 53]. In the future, the training of the neural network will continue and the methodology for image quality pre-processing will be improved: noise reduction, which will significantly increase the efficiency of the neural network, as well as the need to cut the image by a certain pixel size, rather than bringing it to this value as a whole [36, 47, 50].

Conclusions

To solve the problem of classification of color changes in volutinous granules and segmentation of S. cerevisiae yeast cells during the metachromatic reaction, two Python programs were developed using the architecture of artificial neural networks Inception v3 and Unet, and it was found that the architecture of Inception v3 networks is less effective in performing the task of cell segmentation, and the neural network based on the Unet architecture is optimal.

The cells classified by color and the presence of segmentation were counted using a nonrecursive markup algorithm and it was found that the relative error of the created software does not exceed 4.53% and averages 3.85%. The use of this neural network algorithm allows us to more effectively determine the dynamics of the metachromatic reaction under the influence of geophysical factors in an automatic mode.

An accurate and quick assessment of both the number of cells and differences in the metachromasia reaction color of volutin granules of *Saccharomyces cerevisiae* yeast as an effective processing code for metachromatic staining is essential not only for searching biological problems but also for interdisciplinary research.

Funding: This research received no external funding. The only funding was dedicated to mobility which has not materialized because of COVID 19 and War in Ukraine.

Acknowledgments: the article preparation was supported by a bilateral inter-academic mobility project between Ukrainian and Slovak Academies of Science: Geophysical events and their bio indication using microorganisms.

Conflicts of Interest: The authors declare no conflict of interest.

References

1. Chizhevsky A. L. The Terrestrial Echo of Solar Storms. Moscow: Mysl;1976. 366 p.
2. Vladimirsky B. M., Temuryants N. A.. Influence of Solar Activity on the Biosphere - the noosphere: Heliobiology from A. L. Chizhevski to present day. Moscow: MNEPU Publishing House; 2000. 374 p.
3. Gray L. J., Beer J., Geller M., Haigh J. D., Lockwood M., Matthes K., et al. Solar Influences on Climate. Rev. Geophys. 2010;48. RG4001.
4. Gromozova E., Voychuk S., Grigoriev P., Vishnevsky V., Ragulskaya M. Cosmic rays as bio-regulator of deep time terrestrial ecosystems. Sun and Geosphere. 2012; 7(2): 177–20.
5. Gromozova E. N., Kachur T. L., Voychuk S. I., Kharchuk M. S. Research of Metachromatic Reaction of Saccharomyces cerevisiae. Microbiol J., 2016; 78(3), 45-51.
doi: https://doi.org/10.15407/microbiolj78.03.045
6. Gromozova E. N., Voychuk S. I., Zelena L. B., Gretskey I. A. Microorganisms as a model system for studying the biological effects of electromagnetic non-ionizing radiation. INVITED PAPERS; 2012. 137 p. DOI: 10.7562/SE2012.2.02.06
7. Marynchenko L. V., Nizhelska I., Shirinyan A., Makara V. Prospects of using biological test-systems for evaluation of effects of electromagnetic fields. Innovative biosystems & bioengineering. 2019; 3(2): 114-24.
8. Kharchuk M. S., Grigoriev P. E., Kachur T. L., Gromozova E. N. Properties of Saccharomyces cerevisiae volutin granules under conditions of the change of space weather. Microbiol J; 2016; 78(4): 71-81.

9. Kharchuk M. S., Gromozova E. N. Wastewater components effect on metachromasia reaction of volutin granules in vitro. Biotechnologia Acta, 2017; 10(6): 28-34.

10. Gromozova E. N., Grigoriev P. E., Kachur T. L., Voychuk S. I. The influence of cosmophysical factors on the metachromasia reaction of volutein granules of Saccharomyces cerevisiae. Biophysical processes and biosphere. 2010; 9(2): 67–76.

11. Sridharan G., Shankar A. A. Toluidine blue: A review of its chemistry and clinical utility. J of Oral & Maxillofacial Pathology. 2012; 5(41): 57-71.

12. Serafim L. S., Lemos P. C., Levantesi C., Tandoi V., Santos H., Reis M. A. M. Methods for detection and visualization of intracellular polymers stored by polyphosphate accumulating microorganisms.
J Microbiol Methods. 2002; 51(1):1–18.
DOI: 10.1016/s0167–7012(02)00056–8.

13. Gromozova O. M., Kachur T. L., Vishnevsky V. V., Sychev O. S. Information Technology of Color Imaging Assessment of Saccharomyces cerevisiae UCM Y-517 Yeast Volutin Granules. Microbiol J. 2020; 82(5):30-35.
DOI: https://doi.org/10.15407/microbiolj82.05.030.

14. Rogacheva S. M., Otradnova M. I., Zhutov A. S. The cell response to the effect of heliogeophysical factors and extremely high frequency radiation of low intensity. IOP Conf: Ser Earth Environ. 2021; Sci. 853 012020 doi. 10.1088/1755-1315/853/1/012020

15. Bergeron J. A., Singer M. Metachromasy: an experimental and theoretical reevaluation. J of Cell Biology.1958; 4(4): 433-57.
https://doi.org/10.1083/jcb.4.4.433

16. Schubert M., Hamerman D. Metachromasia; chemical theory and histochemical use. J of Histochemistry & Cytochemistry. 1956; 4(2): 159-89.

17. D'Mello PAX, Vijay S. T., Ramya V., Britto F. P., et al. Metachromasia and metachromatic dyes: a review. Int J Adv Health Sci. 2016; 2(10), 12-7.

18. Kramer H., Windrum G. M. The metachromatic staining reaction. J of Histochemistry & Cytochemistry. 1955; 3(3): 227-37.

19. Kharchuk M. S., Gromozova E. N. The Effect of Phosphorus Metabolism on the Motion of Saccharomyces cerevisiae Volutin Granules. Microbiol J. 2021; 83(3):46-55.
DOI: https://doi.org/10.15407/microbiolj83.03.046

20. Widra A. Metachromatic granules of microorganisms. J of Bacteriology. 1959; 78(5): 664-70.

21. Lichko L. P., Kulakovskaya T. P., Kulaev I. S. Inorganic polyphosphates and exopolyphosphatases in different cell compartments of Saccharomyces cerevisiae. Biochem. 2006 Nov;71(11):1171-5.
DOI: 10.1134/s0006297906110010.

22. Najjar YM, Basheer IA, Hajmeer MN. Computational neural networks for predictive microbiology: I. Methodology. Int J of food microbiology. 1997; 34(1): 27-49.

23. Almeida J. S., Noble P. A. Neural computing in microbiology. J of microbiol methods. 2000, 43(1): 1-2.

24. Basheer I. A., Hajmeer M. Artificial neural networks: fundamentals, computing, design, and application. J of microbiol methods. 2000; 43(1): 3-31.

25. Zhang J., Li C., Yin Y., Zhang J., Gregorzek M. Applications of artificial neural networks in microorganism image analysis: a comprehensive review from conventional multilayer perceptron to popular convolutional neural network and potential visual transformer. Artificial Intelligence Rev. 2023; 56(2): 1013-70.

26. Kulaev I. S., Vagabov V. M., Kulakovskaya T. V. High molecular inorganic polyphosphates: biochemistry, cell biology and biotechnology. Moscow: Scientific World; 2005. 216 p.

27. Pal M. K., Mandal N. Induction of metachromasia and circular dichroism in the dye 1, 9-dimethyl methylene blue by ATP. Indian J of Biochemistry & Biophysics. 1990; 27(2): 108-11.

28. Martinez H. C., Martinez J. A., Cosano G. Z., Garcia-Gimeno R. M. Optimization of computational neural network for its application in the prediction of microbial growth in foods. Food sci and technology inter. 2001; 7(2): 159-63.

29. Huang Y., Kangas L. J., Rasco B. A. Applications of artificial neural networks (ANNs) in food science. Critical reviews in food science and nutrition. 2007; 47(2): 113-26.

30. Hajmeer M., Basheer I. A probabilistic neural network approach for modeling and classification of bacterial growth/no-growth data. J of microbiol methods. 2002; 51(2): 217-26.

31. Chollet F. Keras: The Python Deep Learning library; Keras Io. 2015. 327 p.

32. Brownlee J. Deep learning with Python: develop deep learning models on Theano and TensorFlow using Keras; Machine Learning Mastery; 2016. 231 p.

33. Ketkar N., Santana E. Deep learning with Python. Berkeley, CA: Apress; 2017.

34. Szegedy C., Vanhoucke V., Ioffe S., Shlens J., Wojna Z. Rethinking the inception architecture for computer vision. Proceedings of the IEEE conference on computer vision and pattern recognition. 2017. 2818-26. DOI. 10.1109/CVPR.2016.308.

35. Jeon Y., Kim J. Active convolution: Learning the shape of convolution for image classification. Proceedings of the IEEE conference on computer vision and pattern recognition. 2017. 4201-09.
DOI. 10.1109/CVPR.2016.461.

36. Oquab M., Bottou L., Laptev I., Sivic J. Learning and transferring mid-level image representations using convolutional neural networks. Proceedings of the IEEE conference on computer vision and pattern recognition. 2014. 1717-24.

37. Chollet, F. Xception: Deep learning with depthwise separable convolutions. Proceedings of the IEEE conference on computer vision and pattern recognition. 2017. 1251-58.

38. Latha Y. M., Rao B. S. A Systematic Review on Background Subtraction Model for Data Detection. Pervasive Computing and Social Networking: Proceedings of ICPCSN 2021; 341-9.

39. Mihaylov S. R., Ives Z. G., Guha S. REX: Recursive, delta-based data-centric computation. arXiv preprint arXiv:1208.0089; 2012.

40. Fang W., Zhong B., Zhao N., Love PED, et al. A deep learning-based approach for mitigating falls from

height with computer vision: Convolutional neural network. Advanced Engineering Informatics. 2019; 39: 170-7. https://doi.org/10.1016/j.aei.2018.12.005.

41. Dhall I., Vashisth S., Aggarwal G. Automated hand gesture recognition using a deep convolutional neural network model. 10th Inter Conf on Cloud Computing, Data Science & Engineering (Confluence); IEEE. 2020. 811-6.

42. Nikolenko S. Y., Kaduryn A. A., Arkhangelskaya E. O. Deep learning. Dive into the world of neural networks Moskow., Nauka; 2018. 273 p.

43. Gopalakrishnan K., Khaitan S. K., Choudhary A., Agrawal A. Deep convolutional neural networks with transfer learning for computer vision-based data-driven pavement distress detection. Construction and building materials. 2017. 157: 322-330.

44. Ahlswede S., Asam S., Roeder A. Hedgerow object detection in very high-resolution satellite images using convolutional neural networks. J of Applied Remote Sensing. 2021; 15(1): 018501-018507.

45. Laina I., Rupprecht C., Belagiannis V., Tombari F., Navab N. Deeper depth prediction with fully convolutional residual networks. Fourth inter conf on 3D vision (3DV): IEEE; 2016. 239-248. http://doi.org/10.48550/arXiv.1606.00373.

46. Zhou J., Troyanskaya O. G. Predicting effects of noncoding variants with deep learning–based sequence model. Nature methods. 2015, 12(10): 931-4.

47. Jeon Y., Kim J. Active convolution: Learning the shape of convolution for image classification. Proceedings of the IEEE conference on computer vision and pattern recognition. 2017. 4201-9.

48. Huang G., Chen D., Li T., Wu F., et al. Multi-scale dense convolutional networks for efficient prediction. arXiv Forum, preprint arXiv:1703.09844. 2017. 2.2.

49. McNeely-White D., Beveridge J. R., Draper B. A. Inception and ResNet features are (almost) equivalent. Cognitive Systems Research. 2020; 59: 312-8.

50. Purkait N. Hands-On Neural Networks with Keras: Design and create neural networks using deep learning and artificial intelligence principles. Packt Publishing Ltd; 2019.

51. Xue Y., Ray N., Hugh J., Bigras G. Cell counting by regression using convolutional neural network. Computer Vision–ECCV 2016 Workshops: Amsterdam, Oct 8-10: Proceedings; Part I. 14: Springer Intern Publishing; 2016. 274-90.

52. Kalinichenco E. O., Hretskyi I. O., Gorgo Y. P. Use of neuron networks models in biotechnology. XIV Conf. «Biotechnology of XXI century». Kyiv: Igor Sikorsky's KPI; 2020. 122.

53. Gorgo Y. P., Kotseruba A. S. Using neural networks to assess the metachromatic reaction of yeast volutin granules. II Inter science and pract conf Theory and practice of current scientific research. Odesa;2018.33-5.

54. Ghanbari B., Atangana A. A new application of fractional Atangana–Baleanu derivatives: designing ABC-fractional masks in image processing. Physica A: Statistical Mechanics and its Applications; 2020. 542: 123516.

55. Livathinos N., Berrospi C., Lysak M., Kuropiatnyk V., et al. Robust PDF document conversion using recurrent neural networks. Proceedings of the AAAI Conf on Artificial Intelligence. 2021. 15137-45.

The article has been sent to the editors 18.05.24.
After processing 10.06.24.
Submitted for printing 28.06.24.